Stem Cell Research 25 (2017) 166–178

Contents lists available at ScienceDirect

Stem Cell Research

journal homepage: www.elsevier.com/locate/scr

Multiple intracerebroventricular injections of human umbilical cord mesenchymal stem cells delay motor neurons loss but not disease progression of SOD1G93A mice

Francesca Sironi [a], Antonio Vallarola [a], Martina Bruna Violatto [b], Laura Talamini [b], Mattia Freschi [a], Roberta De Gioia [a], Chiara Capelli [c], Azzurra Agostini [d], Davide Moscatelli [d], Massimo Tortarolo [a], Paolo Bigini [b], Martino Introna [c], Caterina Bendotti [a,*]

[a] Department of Neuroscience, IRCCS — Istituto di Ricerche Farmacologiche "Mario Negri", Milano, Italy
[b] Department of Biochemistry and Molecular Pharmacology, IRCCS — Istituto di Ricerche Farmacologiche "Mario Negri", Milano, Italy
[c] USS Center of Cellular Therapy"G. Lanzani", ASST Papa Giovanni XXIII, Bergamo, Italy
[d] Department of Chemistry, Material and Chemical Engineering "G. Natta", Politecnico di Milano, Milano, Italy

ARTICLE INFO

Article history:
Received 31 March 2017
Received in revised form 2 November 2017
Accepted 4 November 2017
Available online 10 November 2017

Keywords:
Max 6
Amyotrophic lateral sclerosis
Mesenchymal stem cells
Umbilical cord
Transgenic SOD1G93A mice
Motor neuron
Gliosis

ABSTRACT

Stem cell therapy is considered a promising approach in the treatment of amyotrophic lateral sclerosis (ALS) and mesenchymal stem cells (MSCs) seem to be the most effective in ALS animal models. The umbilical cord (UC) is a source of highly proliferating fetal MSCs, more easily collectable than other MSCs. Recently we demonstrated that human (h) UC-MSCs, double labeled with fluorescent nanoparticles and Hoechst-33258 and transplanted intracerebroventricularly (ICV) into SOD1G93A transgenic mice, partially migrated into the spinal cord after a single injection. This prompted us to assess the effect of repeated ICV injections of hUC-MSCs on disease progression in SOD1G93A mice. Although no transplanted cells migrated to the spinal cord, a partial but significant protection of motor neurons (MNs) was found in the lumbar spinal cord of hUC-MSCs-treated SOD1G93A mice, accompanied by a shift from a pro-inflammatory (IL-6, IL-1β) to anti-inflammatory (IL-4, IL-10) and neuroprotective (IGF-1) environment in the lumbar spinal cord, probably linked to the activation of p-Akt survival pathway in both motor neurons and reactive astrocytes. However, this treatment neither prevented the muscle denervation nor delayed the disease progression of mice, emphasizing the growing evidence that protecting the motor neuron perikarya is not sufficient to delay the ALS progression.

1. Introduction

Amyotrophic lateral sclerosis (ALS) is an adult-onset fatal neurodegenerative disorder characterized by the degeneration of motor neurons in the brain and spinal cord, leading progressively to muscle weakness, paralysis and finally death for respiratory failure within 3–5 years from the diagnosis (Cleveland and Rothstein, 2001; Rowland and Shneider, 2001). Almost 90% of ALS cases are sporadic, while 10% are familial, due to mutations in several genes (Kiernan et al., 2011). Mutation in the gene coding for SOD1, the first discovered, has led to the development of animal models of the disease, among which that carrying the SOD1G93A is the most studied since better reproduce the phenotype of ALS (Bendotti and Carrì, 2004). Riluzole, which has been approved by Food and Drug Administration >15 years ago, remains so far the unique pharmacological treatment showing a modest effect in delaying the survival of patients by 3–6 months and of about 10 days in mouse models. This paucity in therapy is likely due to the multifaceted nature of ALS which involves different pathogenic mechanisms and various non-neuronal cells including glial and immune cells which can play either neurotoxic or neuroprotective action depending on their state of activation.

Recently, stem cell therapy has emerged as a promising approach for several neurological disease treatment, including ALS (Adami et al., 2014). Not only neural stem cells but also other cell types like mesenchymal stem cells (Lewis and Suzuki, 2014), umbilical cord blood stem cells (Garbuzova-Davis et al., 2012), glial-restricted progenitor cells

Abbreviations: ALS, amyotrophic lateral sclerosis; SOD1, superoxide dismutase 1; MSCs, mesenchymal stem cells; UC, umbilical cord; h, human; NP, nanoparticles; ICV, intracerebroventricular; CNS, central nervous system; NTG, non-transgenic; PBS, phosphate buffer solution; TAM, tibialis anterior muscle; GFAP, glial fibrillary acidic protein; IBA1, Ionized calcium-binding adapter molecule; NMJ, neuromuscular junction; MNs, motor neurons; IL-1β, interleukin 1β; IL-4, interleukin 4; IL-6, interleukin 6; IL-10, interleukin 10; IGF-1, insulin growth factor 1.

* Corresponding author at: Laboratory of Molecular Neurobiology, Department of Neuroscience, IRCCS - Istituto di Ricerche Farmacologiche Mario Negri, Via La Masa, 19, Milan 20156, Italy.
E-mail address: caterina.bendotti@marionegri.it (C. Bendotti).

https://doi.org/10.1016/j.scr.2017.11.005

(Kruminis-Kaszkiel et al., 2014) have exerted positive effects in rodent models of ALS. Their mechanism of action is not due to the substitution of degenerating motor neurons, but rather to the creation of a protective milieu near the motor neurons through secretion of neuroprotective factors and the reduction of neuroinflammation (Coatti et al., 2015). The promising results from preclinical studies prompted several early-phase clinical trials with hMSCs aimed to establish the safety of the treatment and delivery method (Glass et al., 2016; Mazzini et al., 2015).

The human umbilical cord (hUC) is a viable source of mesenchymal stem cells (MSCs), which can be collected easily, in a painless manner and without ethical concerns because umbilical cord is a discarded tissue (Watson et al., 2015). hUC-MSCs hold a high proliferative rate, are immunoprivileged thanks to the low expression of MHCI molecules and the absence of MHCII expression which avoid their rejection (Todeschi et al., 2015). Moreover, they secrete diverse trophic factors and cytokines and display strong anti-inflammatory and immunomodulatory capacities (Koh et al., 2008; Lund et al., 2007). For all these reasons, the use of hUC-MSCs could be more advantageous and beneficial than the MSCs from other sources.

In a previous study, we observed that labeled hUC-MSCs, administered by a single intravenous bolus, accumulated in lungs but they migrate neither in the brain nor spinal cord and were rapidly removed from filter organs in about 24 h (Violatto et al., 2015). On the contrary, when they were transplanted into cerebral ventricles (ICV), although most of them remained confined to the site of injection, few were found in the spinal cord of SOD1G93A mice especially one week after transplantation (Violatto et al., 2015). This distribution was similar to that found after a single ICV injection of human umbilical cord blood which produced a modest amelioration of the disease progression in SOD1G93A and wobbler mice suggesting a bystander mechanism through the secretion of neurotrophic factors (Bigini et al., 2011). Thus, in the present study, to enhance the probability of cell migration and the effect of secreted factors in all the spinal cord segments we decided to perform repeated ICV injections of hUC-MSCs and to examine their distribution and their effect on disease progression and neuropathology in SOD1G93A mice. Treatment with MSCs from bone marrow improved motor performances and prolonged the survival of transgenic SOD1G93A mice when administered intravenously, starting at the early presymptomatic phase (Zhao et al., 2007), or at the onset (Uccelli et al., 2012) of disease. In addition human MSCs act preventively on the disease onset if transplanted into the spinal cord (Vercelli et al., 2008) or delivered intrathecally (Kim et al., 2010). Here we decided to start the transplantation when the mice exhibit the first sign of disease, i.e. the interruption of body weight growth compared to their non-transgenic littermates which occurs around 98 days of age (Caron et al., 2015) a condition more consistent with the therapeutic approach in ALS sporadic patients. We injected the hUC-MSCs into lateral ventricles once every two weeks up to three times in total and we examined their accumulation and distribution in the CNS using fluorescent nanoparticles as previously made. In parallel we assessed their effect on motor neuron degeneration in the lumbar spinal cord, muscle denervation, disease progression and survival of SOD1G93A mice. We demonstrated that even after repeated ICV injections, hUC-MSCs remained confined to the cerebral ventricles and did not migrate into the spinal cord of mutant SOD1 mice. However, they were able to partially protect the motor neuron and reduce microglia activation in the lumbar spinal cord suggesting a bystander action through the secretion of neuroprotective factors. Nevertheless, this effect was not associated with the prevention of limb muscle denervation or with a slowing of disease progression.

2. Methods

2.1. Human UC-MSCs cultures

Fresh human UC were collected from the Operating Room of the Obstetrics and Gynecology Unit at ASST Papa Giovanni XXIII in Bergamo (Italy). Informed written consent was obtained from each donor mother according to the guidelines of ethical committee of the ASST Papa Giovanni XXIII, as required by the clinical trial "Umbilical Cord Derived Mesenchymal Stromal Cells For The Treatment of Severe Steroid-resistant Graft Versus Host Disease" (ClinicalTrials.gov Identifier: NCT02032446) approved by "Istituto Superiore di Sanità" and "Agenzia Italiana del Farmaco". After cesarean sections, UC-MSCs have been isolated from the whole UC by tissue mechanical disaggregation and cultivated, as previously described (Capelli et al., 2015). Briefly, the UC was cut into 5 cm long segments which were longitudinally cut and split open to expose the inner surface. Each UC segment, subsequently minced in very small fragments, was transferred into 150 mm cell culture Petri dishes (Corning) containing MSC expansion medium consisting of alpha-Minimum Essential Medium (MEM) (Life-Technologies) enriched with 5% human platelet lysate obtained from healthy donors, 50 μg/ml gentamicin (Fisiopharma) and 2 UI/ml Heparin (Hospira). They were maintained at 37 °C in a humidified atmosphere with 5% CO_2 for 6–7 days after which the UC tissue was removed and the adherent cells were allowed to expand for an additional week. After approximately 14 days, the adherent cells were harvested by TrypLe Select 1X (Life-Technologies) treatment and re-plated in T175 flasks (BD Falcon) in MSC expansion medium for further expansion. Immunophenotype analysis and multilineage differentiation potential of cells have been extensively characterized (Capelli et al., 2011).

2.2. Nanoparticle synthesis and cell labeling

Poly (methyl methacrylate) nanoparticles (from now on referred to as NPs) were obtained from a copolymerization between methyl methacrylate (MMA) and a macromonomer of 2-hydroxyethyl methacrylate covalently bound to Rhodamine b (RhB). This process avoids the dispersion of dyes and the consequent risk of biological elution, as previously described (Dossi et al., 2013). For cell tracking experiment, UC-MSCs were incubated with 200 nm RhB-positive NPs with a concentration of 1.25×10^{10} NPs/ml for 48 h and Hoechst 33258 (4 μg/ml) for 12 h as previously described (Bigini et al., 2016; Violatto et al., 2015).

2.3. Animals and treatment

Female adult transgenic SOD1G93A mice on C57BL6/J background were used in this study as male mice are normally used for breeding to maintain the colony. All animals were housed under SPF (specific pathogen free) conditions at a temperature of 22 ± 1 °C, relative humidity of 55 ± 10% and 12 h light/dark schedule, 5 per cage. Food (standard pellets) (Altromin, MT, Rieper) and water were supplied ad libitum. Procedure involving animals and their care were conducted in according to the institutional guidelines, that are in compliance with national (D.lgs 26/2014; Authorization n.19/2008-A issued March 6, 2008 by Ministry of Health) and international laws and policies (EEC Council Directive 2010/63/UE; NIH Guide for the Care and use of Laboratory Animals, U.S. National Research Council, 2011 edition). This specific protocol was approved by IRCCS-IRFMN Animal Care and Use Committee (IACUC) and then approved by the Italian "Istituto Superiore di Sanità" (code: No 1131/2015 PR).

Mice SOD1G93A ($n = 58$) of 98 days of age were randomly assigned to different experimental groups, so that the mean body weight was similar between groups. For histological, biochemical and behavioral analyses 46 SOD1G93A mice were recruited, while for ex vivo cell tracking analysis 12 SOD1G93A mice were used. Non-transgenic age matched mice (NTG) ($n = 13$) were recruited as control for both histological and biochemical analysis. The experimental schedule is reported in Table 1.

The 46 SOD1G93A mice enrolled for the evaluation of hUC-MCSs effectiveness were further divided into two groups: the first ($n = 23$) receiving 250,000 hUC-MSCs resuspended in 8 μl of sterile PBS into the lateral cerebral ventricles, the second ($n = 23$) receiving the same volume of sterile PBS (vehicle). The experimental group composed of 12

Table 1
Experimental groups for in vivo analyses. L = labelled; d = days of age; d = day; X = sacrifice.

			14 w	14 w + 1 d	16 w	18 w	20 w	End stage	
SOD1G93A	UC-MSCs	$n = 8$	ICV		ICV	ICV	X		Biochemistry histology
SOD1G93A	PBS	$n = 8$	ICV		ICV	ICV	X		
SOD1G93A	UC-MSCs	$n = 15$	ICV		ICV	ICV	ICV	X	Behavior
SOD1G93A	PBS	$n = 15$	ICV		ICV	ICV	ICV	X	
SOD1G93A	L UC-MSCs	$n = 3$	ICV	X					Cell tracking
SOD1G93A	L UC-MSCs	$n = 3$	ICV				X		
SOD1G93A	L UC-MSCs	$n = 3$	ICV		ICV	X			
SOD1G93A	L UC-MSCs	$n = 3$	ICV		ICV	ICV	X		

SOD1G93A mice received the same amount of NPs/Hoechst-33258 labeled hUC-MSCs.

To avoid an excessive load in a single ventricle, 4 μl were injected for each side. Animals received an intraperitoneal (ip) injection of the analgesic Buprenorphine (100 mg/kg) dissolved in sterile saline solution before the surgical procedure. They were anesthetized with a 5% isoflurane/oxygen mixture. The following stereotaxic coordinates were used (anterior-posterior 0.0 mm from the bregma; lateral ± 1.0 mm from the bregma; deepness −3.0 mm from skull surface).

For histological and biochemical analyses, 16 mice (PBS $n = 8$; hUC-MSCs $n = 8$) received 3 ICV injections, once every 14 days (98, 112 and 126 days of age) and then sacrificed at 140 days of age, when usually SOD1G93A mice show about 50% reduction in their motor performance on Rota-Rod (symptomatic stage).

For the behavioral tests, 30 mice (PBS $n = 15$; hUC-MSCs $n = 15$) received 4 ICV injections once every 14 days (98, 112, 126and 140 days of age) and were euthanized at the end stage of the disease considered when the mice were unable to right themselves within 10 s after being placed on their sides. The 12 SOD1G93A mice enrolled for cell tracking study were divided into the following four subgroups: 1) $n = 3$ mice were sacrificed 24 h after the first ICV injection; 2) $n = 3$ mice were sacrificed 6 weeks after the first ICV injection (140 days of age); 3) $n = 3$ mice were sacrificed 2 weeks after the second ICV injection (126 days of age); 4) $n = 3$ mice sacrificed 2 weeks after the third ICV injection (140 days of age). ICV injections were performed with a gap of 2 weeks between each other. At the end of the study, brain and spinal cord were immediately collected and frozen in liquid nitrogen, to ensure optimal quality of tissues. Sections (30 μm) were obtained after cryostat cutting and observed with a BX81 microscope equipped with an F-view II CDD camera (Olympus).

2.4. Disease progression assessment

The disease progression was evaluated in all mice (PBS $n = 15$; hUC-MSCs $n = 15$), twice a week from the start of the experiment, by an operator blinded to the treatment. The parameters measured included body weight, latency to fall from the Rota-Rod and from the grid (grip strength) as previously described (Tortarolo et al., 2015). Body weight was monitored before behavioral tests and immediately before and after the surgery and as well as the day after to ensure that the mice tolerated the procedure without major surgical complications, such as injection-attributable neurological worsening. The Rota-Rod test was performed using the Rota-Rod apparatus (model 7650, Ugo Basile). The animals were placed on the rotating bar with a constant acceleration of 4 rotations per minute (rpm) starting from a speed of 7 rpm up to 28 rpm for a maximum of 300 s. The latency to fall was recorded and the test was repeated for a maximum of three times interspersed by 5 min rest between sessions. For the grip strength test to measure the limb resistance, mice were placed on a horizontal metallic grid that was slightly shaken to force the mouse grip and then inverted. The latency to fall of each mouse was recorded. The test ended after 90 s; in the case of failure, the measurement was repeated three times. The best performance of the sessions was considered for the statistical analysis.

2.5. Histological examination

For histological analyses, 12 mice (NTG $n = 4$; PBS $n = 4$; hUC-MSCs $n = 4$) at the symptomatic stage of the disease and 15 mice (NTG $n = 5$; PBS $n = 5$; hUC-MSCs $n = 5$) at the end stage were deeply anesthetized with ketamine hydrochloride (150 mg/kg) and medetomidine (2 mg/kg) followed by intracardiac perfusion with 4% paraformaldehyde (PFA, Merck) in PBS 0.1 M, pH 7.4. Spinal cords were removed and post-fixed for 24 h in 4% PFA in PBS 0.1 M (Tortarolo et al., 2015). Tissues were dehydrated in 30% sucrose solution in PBS until they sank, embedded in cryostat medium OCT (Sakura, Zoeterwounde, The Netherlands) and then frozen in N-pentane at −45 °C for 3 min and conserved at −80 °C. Thirty micrometre coronal sections were obtained by cutting lumbar spinal cords (L2–L5) using a cryostat at −20 °C. The spinal cord sections were collected in PBS 0.01 M and transferred in a cryo-preservative solution (NaH_2PO_4, Na_2HPO_4, MilliQ H_2O, Ethylene Glycol, Glycerol) and stored at −20 °C until use. For the evaluation of the NMJ denervation according to the previously described protocol (Tortarolo et al., 2015), tibialis anterior muscles (TAM) were dissected and snap-frozen in cooled isopentane. Sagittal sections (20 μm) were obtained using a cryostat at −20 °C; they were then placed on a polylisinate glass and stored at −20 °C until use.

2.5.1. Nissl staining and motor neuron counts

For motor neuron counting, 20 serial coronal sections (1 every 10) from lumbar spinal cord per animal were Nissl-stained as previously described (Peviani et al., 2014). Motor neuron counting was performed at 10× magnification using the free software ImageJ (http://imagej.nih.gov/ij/), previously calibrated. Only the large polygonal neurons with a cell body area ≥ 400 μm^2, with a clear nucleolus and a distinctly labeled Nissl-dense cytoplasm, located in a congruent position were incorporated into the counts. The number of motor neurons was calculated for each hemisection and the means used for statistical analysis.

2.5.2. Immunofluorescence of lumbar spinal cord

Immunofluorescence was evaluated on 6 coronal spinal cord slides (1 every 10) from lumbar spinal cord per animal. After blocking the non-specific binding sites by incubation with a solution containing normal goat serum (NGS 10%) and Triton (0.3%) in PBS 0.01 M, the sections were incubated with the primary antibodies (overnight at 4 °C), diluted in a solution containing NGS and Triton in PBS 0.01 M: mouse monoclonal anti-GFAP (1:2500, Merk Millipore), rabbit anti-IBA1 (1:500, Wako) mouse anti-SMI-31 (1:1000, Sternberger Inc.). After three washes in PBS 0.01 M, the sections were incubated (1 h at room temperature) with appropriate secondary antibodies conjugated with a fluorophore (Alexa Fluor® Dyes, Life Technologies), diluted (1:500) in a solution containing NGS (1%) in PBS 0.01 M: Alexa 488 anti-mouse, Alexa 488 anti-rat and Alexa 647 anti-rabbit. Then after 3 washes in PBS 0.01 M, the sections were mounted on glass slides and then covered with coverslips using FluorSaveTM (Calbiochem). The quantification of GFAP and IBA1 intensity was carried out by the same operator blinded to treatment, by determining the mean gray value of fluorescent signals in the ventral horns in the relative surface occupied by the staining. The

quantification was performed at 20× magnification for GFAP and IBA1 immunostaining and 40× magnification for SMI-31 immunostaining, using the free software ImageJ (http://imagej.nih.gov/ij/). Immunofluorescence for SMI-31 was performed with same protocol used for GFAP and IBA1 using as primary antibody mouse anti-SMI-31 (1:1000, Sternberger Inc.).

2.5.3. Immunohistochemistry of p-Akt

Endogenous peroxidases were inactivated by 1% hydrogen peroxide in TBS (0.1 M Tris–HCl, 0.14 M NaCl, pH 7.4). The sections were then incubated with 3% bovine serum albumin (BSA) in TBS/Triton 0.1% 1 h at RT, and then probed overnight at 4 °C in 3% BSA, TBS/Triton with an anti-p-Akt rabbit polyclonal antibody, 1:500 dilution, from Cell Signaling. Subsequently, the sections were washed in TBS/Triton and incubated 1 h at RT in 1% BSA, TBS with a secondary biotinylated anti-rabbit antibody, 1:200 dilution, from Vector. The secondary antibody was revealed with a TSA amplification kit, Cy5 (Perkin Elmer) as previously described (Peviani et al., 2007).

For each immunofluorescence procedure, some of the sections were processed without primary antibody, to verify the specificity of the staining.

2.5.4. Neuromuscular junctions (NMJs)

Detection of the NMJ denervation was made in five non consecutive sagittal sections of TAM. Slices were fixed in acetone for 10 min, incubated in a blocking solution (0.3% Triton, 10% NGS in 0.01 M PBS) for 1 h at 22 °C and then left overnight at 4 °C with anti-synaptophysin primary antibody (rabbit, 1:100, Synaptic System) in 0.15% Triton, 5% NGS, 0.01 M PBS. The sections were then incubated with goat anti-rabbit 647 (1:500, Alexa Fluor® Dyes, Life Technologies) secondary antibody and with bungarotoxin (1:500, Invitrogen) conjugated with Alexa Fluor® 594 (Life Technologies). Dual-staining co-localization of pre and post-synaptic markers was analyzed at 20× magnification under an Olympus Fluoview confocal microscope (FV1000). Innervated neuromuscular junctions were identified by totally or partially co-localization of synaptophysin with bungarotoxin. Plaques marked with bungarotoxin only were considered denervated and they were expressed as the percentage of the total plaques (counted in 8 adjacent frames per section).

2.6. Western blot

The lumbar spinal cord (NTG = 4; PBS = 4; hUC-MSCs = 4) was rapidly dissected and processed as previously described (Tortarolo et al., 2015). The tissue was homogenized by sonication in ice-cold homogenization buffer (20 mM Tris-HCl pH 7.4, 2% Triton X-100 1%, 150 mM NaCl, 1 mM EDTA, 5 mM $MgCl_2$, anhydrous glycerol 10%, protease and phosphates inhibitor cocktail, Roche), centrifuged at 13,000 rpm for 30 min at 4 °C. Proteins from supernatant were separated by electrophoresis on polyacrylamide gels and transferred onto polyvinylidene difluoride (PVDF) membranes. Blots were probed with primary antibodies, mouse monoclonal anti-GFAP (1:1000, Millipore), rabbit polyclonal anti-IBA1 (1:1000, Wako); rabbit monoclonal anti-p-Akt (1:750, Cell Signaling); anti-Akt, (1:1000, Cell Signaling); mouse monoclonal anti-GAPDH (1:20,000, Millipore), and then with peroxidase-conjugated appropriate secondary antibodies. Blots were developed with Immobilon Western Chemiluminescent HRP Substrate (Millipore) on the Chemi-Doc XRS System (Bio-Rad Laboratories, Hercules, CA, USA).

2.7. Real-time PCR

Spinal cords were freshly collected and frozen on dry-ice. Total RNA from spinal cord was extracted using the Trizol method (Invitrogen) and purified with PureLink RNA columns (Life Technologies). RNA samples were treated with DNase I and reverse transcription was performed with High Capacity cDNA Reverse Transcription Kit (Life Technologies). Real-time PCR was performed using the Taq Man Gene expression assay (Applied Biosystems) following the manufacturer's instructions, on cDNA specimens in triplicate, using 1× Universal PCR master mix (Life technologies) and 1× mix containing specific receptors probes for the interleukin 1 beta (IL-1β, Mm00434228_m1); interleukin 4 (IL-4, Mm00445259_m1); interleukin 6 (IL-6, Mm00446190_m1); interleukin 10 (IL-10, Mm00439614_m1); insulin growth factor1 (IGF-1, Mn00439560_m1). Relative quantification was calculated from the ratio between the cycle number (Ct) at which the signal crossed a threshold set within the logarithmic phase of the given gene and that of the reference β-actin gene (4310881E; Life Technologies). Mean values of the triplicate results for each animal were used as individual data for 2-ΔΔCt statistical analysis.

2.8. Statistical analysis

Statistical analyses were performed using the Prism software (Graph Pad Prism 6, Graph Pad Inc.), USA. Body weight, Rota-Rod test, grip strength test data were analyzed using ANOVA for repeated measures, followed by Tukey's Post Hoc test. Survival analysis was performed by the Log-rank test. For the histological analyses, the data were statistically analyzed using One way ANOVA followed by Tukey's Post Hoc test.

3. Results

3.1. hUC-MSC clusters in the ventricle but do no migrate to spinal cord parenchyma

A representative pattern of hUC-MSC distribution at different time points in the brain of SOD1G93A mice is reported in Fig. 1. In accordance with our previous work (Violatto et al., 2015), clusters of double-labeled hUC-MSCs were largely detected at the level of lateral ventricles strongly associated with the choroid plexus cells (Fig. 1A-B). Six weeks after one single treatment, the size and the number of events forming these cell clusters markedly decreased into lateral ventricles. Interestingly, a signal related to cells was found along more caudal ventricle structures below hippocampus region (Fig. 1C-D).

In order to enhance the accumulation and the therapeutic efficacy of stem cells, multiple treatments were carried out. A comparison between double and triple cell administration is shown in Fig. 1E-F-G-H. In both conditions, UC-MSCs are still located along ventricle structures. An increase of cell clusters was observed close to the site of injection and near hippocampus area compared to animals receiving a single administration (Fig. 1C-D). Cell tracking also revealed that, despite the multiple administrations, hUC-MSCs did not migrate in the brain parenchyma, even close to the ventricles (Fig. 1), and in the spinal cord (not shown).

3.2. hUC-MSC partially prevent the motor neurons loss but not the muscle denervation

Motor neuron (MN) count performed on lumbar spinal cord sections from 140-day-old SOD1G93A mice injected with PBS showed a marked reduction of alpha-motor neuron (≥400 μm^2) compared to non-transgenic littermates and this effect was significantly attenuated in hUC-MSCs-treated SOD1G93A mice (NTG, 17.66 ± 1.20; hUC-MSCs, 10.25 ± 0.60 vs PBS, 7.28 ± 0.29, $p < 0.05$) (Fig. 2D). In addition, also the functionality of motor neuron was ameliorated in 140-day-old SOD1G93A mice treated with hUC-MSCs (Fig. 2E-G). In fact, while in NTG mice (Fig. 2E) the phosphorylated neurofilaments, labeled with SMI-31, were present in neuropil, axon terminals, and dendrites, leaving the perikarya totally unstained in symptomatic SOD1G93A mice, SMI-31 immunofluorescence accumulates in altered neuronal structures, such as vacuolized and dystrophic axons, dendrites and soma, as marker of MN dysfunction (Tortarolo et al., 2003) (Fig. 2F). These aberrant structures were less evident in SOD1G93A mice treated with hUC-MSCs

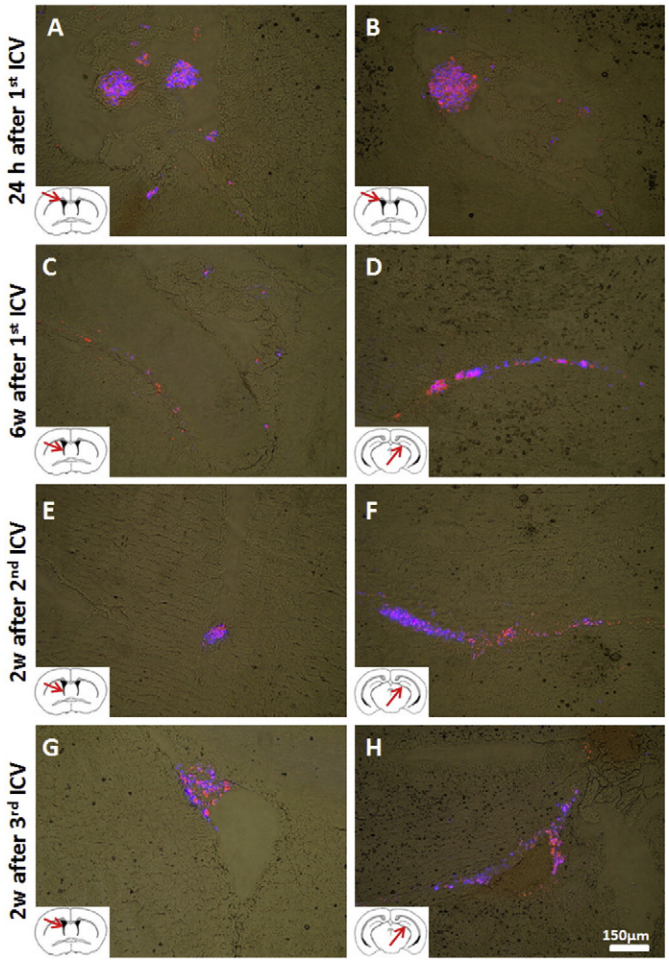

Fig. 1. Double labeled UC-MSCs tracking. Histological brain sections from SOD1G93A mice sacrificed 24 h after the first ICV injection (A-B); 6 weeks after the first ICV injection (C-D); 2 weeks after the second ICV injection (E-F) and 2 weeks after the third ICV injection (G-H). The blue signal is related to the staining of stem cell nuclei with the Hoechst-33258 and the red staining is associated with RhB fluorescent NPs.

(Fig. 2G) confirming the partial preservation of MN cell bodies in the spinal cord.

However, when we analyzed the extent of NMJ denervation of the tibialis anterior muscle of SOD1G93A mice treated with PBS or hUC-MSCs at symptomatic stage (140 days of age) we found no difference in the robust plaque denervation observed when compared to NTG mice (Fig. 3D).

3.3. hUC-MSC reduce the activated microglia but increase the reactive astrocytes in the lumbar spinal cord

It has been suggested that stem cells act as support for dying motor neurons not only by releasing neurotrophic factors but also reducing neuroinflammation in damaged regions. Therefore we evaluated both reactive astrocytosis and microgliosis at the symptomatic stage of the disease, in the lumbar spinal cord of hUC-MSCs treated SOD1G93A mice compared to those treated with PBS. As expected the immunostaining for GFAP, the specific marker of astrocytes was increased in the spinal cord of SOD1G93A mice treated with PBS compared with non-transgenic littermates. Unexpectedly, this effect was significantly exacerbated in hUC-MSCs treated mice ($p < 0.05$), as demonstrated by both immunohistochemistry (Fig. 4A-D) and western blot analysis (Fig. 4E-F). On the contrary, the IBA1 immunostaining, a marker of microglia activation, was significantly reduced in hUC-MSCs treated SOD1G93A mice compared to mice treated with PBS at 140 days age ($p < 0.001$) (Fig. 5A-D). This effect was partially confirmed by the western blot of lumbar spinal cord homogenate (Fig. 5G-F). In fact, the increased levels of Iba1 in SOD1G93A mice compared to NTG were reduced by the treatment with hUC-MSCs although the effect did not reach the statistical significance.

3.4. hUC-MSCs increase the anti-inflammatory cytokine and IGF-1 while reducing the proinflammatory cytokines.

As MSCs has been reported to exert their neuroprotective effect by modulating the inflammatory environment around MNs (Boido et al., 2014) we examined the mRNA levels by real time PCR of pro-inflammatory cytokine (IL-6 and IL-1β) and the anti-inflammatory cytokine (IL-4 and IL-10) in the lumbar spinal cord of hUC-MSCs treated as compared to PBS treated SOD1G93A mice and non transgenic mice. While the levels of IL-6 mRNA show a non significant reduction in SOD1G93A mice treated with PBS with respect to NTG, the levels in hUC-MSCs treated mice were further reduced and significantly different from the NGT mice. The mRNA levels of proinflammatory IL-1β, on the contrary, were increased by about 3 fold in SOD1G93A mice compared to NTG mice while the hUC-MSCs attenuated this effect (Fig. 6B). Much different is the situation for the levels of the anti-inflammatory cytokine IL-4 mRNA, that did not change in SOD1G93A mice treated with PBS but significantly increased of about 8-fold compared to NTG and vehicle-treated transgenic mice (Fig. 6C). Finally, IL-10 mRNA which significantly decreased in SOD1G93A mice treated with PBS compared to NTG mice, showed a mild recovery in the hUC-MSCs treated mice even if not statistically significant (Fig. 6D). Since MSCs were also reported to induce the production of endogenous neuroprotective factors in the host transplanted tissue, we examined the levels of IGF-1 which is known to be a potent survival factor for motor neurons. In line with this, we found a 4-fold increase in mRNA levels of IGF-1 in the spinal cord of SOD1G93A treated with hUC-MSCs compared to mice treated with PBS (Fig. 6E).

3.5. Activation of pro survival pathway in lumbar spinal cord.

In the nervous system activation of the PI3K/Akt pathway is one of the mechanisms specifically involved in neuronal survival and cell proliferation in response to growth factors and cytokine stimulation (Brunet et al., 2001; Peviani et al., 2007). For this reason we wanted to verify if the partial MN protection and the increased astrocytosis observed in the 140-day-old hUC-MSCs treated mice could be linked to the activation of this pathway. According to previous observation (Peviani et al., 2007), no changes in the p-Akt/Akt pathway were detected at the symptomatic stage of the disease between NTG and SOD1G93A treated with PBS by Western Blot, while the p-Akt/Akt ratio significantly improved in the hUC-MSCs-treated group compared to the vehicle and NTG (PBS vs. hUC-MSCs $p < 0.01$) (Fig.7A-B). We also examined the distribution of p-Akt by immunofluorescence in combination with GFAP to determine the cellular distribution of the activated protein and to define whether an increase of astrocytosis could be linked to the activation of this prosurvival pathway. While, in the lumbar spinal cord of NTG mice p-Akt and GFAP did not colocalized, in SOD1G93A mice we observed a partial co-localization of GFAP with p-Akt which was magnified in the lumbar spinal cord sections from hUC-MSC treated mice.

3.6. hUC-MSC do not alter the disease onset, duration and survival ameliorate the disease progression

The trend of body weight change in SOD1G93A mice showed no significant differences between the groups treated with PBS or UC-MSCs (Fig. 8A) indicating a good tolerability of surgical delivery of stem cells and ruling out possible cell toxicity. We can also exclude any behavioral deterioration due to the ICV treatment since the variation of body weight and the grip endurance trend was similar to that reported

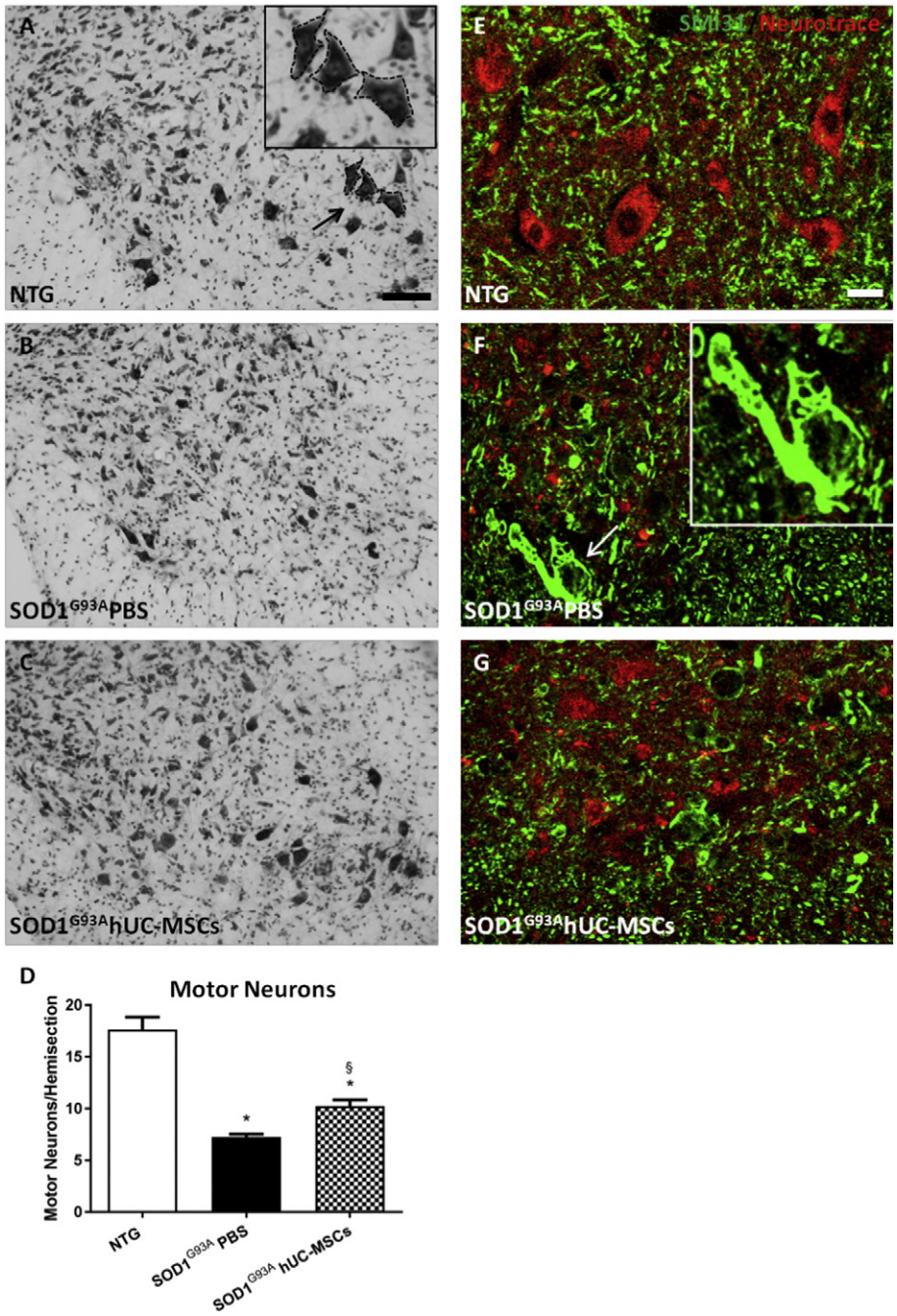

Fig. 2. Motor neuron loss and dysfunction. Motor neurons were counted on Nissl stained lumbar spinal cord hemisections from mice at 140 days of age (A-C), scale bar 100 μm. At the symptomatic stage of the disease motor neurons, with cell body area ≥ 400 μm^2 (arrow, A), resulted significantly decreased in both transgenic group of mice compared to non-transgenic (NTG). Treatment with hUC-MSCs showed a partial but significant neuroprotection (D). The bar graph represents mean ± SEM ($n = 4$ animals); * = $p < 0.0001$ vs NTG; § = $p < 0.05$ vs SOD1G93APBS (One way ANOVA, followed by post-hoc Tukey's test). In lumbar spinal cord of transgenic mice (F), we observed a marked increase of phosphorylated neurofilaments (SMI-31 green, arrow) compared to NTG mice (E), as an index of MNs dysfunction. Treatment with hUC-MSCs reduced the accumulation SMI-31 in the motor neuron cell body labeled with neurotrace (NT, red) and proximal axons (scale bar: 20 μm).

previously from our group in untreated SOD1G93A mice (Tortarolo et al., 2003). Compared with the PBS-treated mice, those treated with hUC-MSCs did not present a better performance on neuromuscular tests, except for a slight, not significant improvement on both Rota-Rod test and grip strength at about 126 days of age, the time point at which the largest number of cells was detected in the cerebral ventricles (Fig. 8B-C). The repeated treatment with hUC-MSCs did not prolonged mice survival (mean: PBS, 170.6 ± 3.3; hUC-MSCs, 174.6 ± 2.5 days). However, when 50% of PBS-treated mice have died, still 75% of the hUC-MSCs treated mice were alive (Fig. 8D) showing a trend to increase life span. We can exclude any behavioral deterioration due to the ICV treatment since the variation of body weight and the grip endurance trend was similar to that reported previously from our group in untreated SOD1G93A mice (Tortarolo et al., 2015).

4. Discussion

MSCs have been considered as a promising tool for the treatment of ALS as they have multipotential features such as the ability to secrete neurotrophic factors and exert an immunomodulatory effect. Different studies have demonstrated the efficacy of MSCs, mostly originating from the bone marrow or adipose tissue, in delaying the onset of the

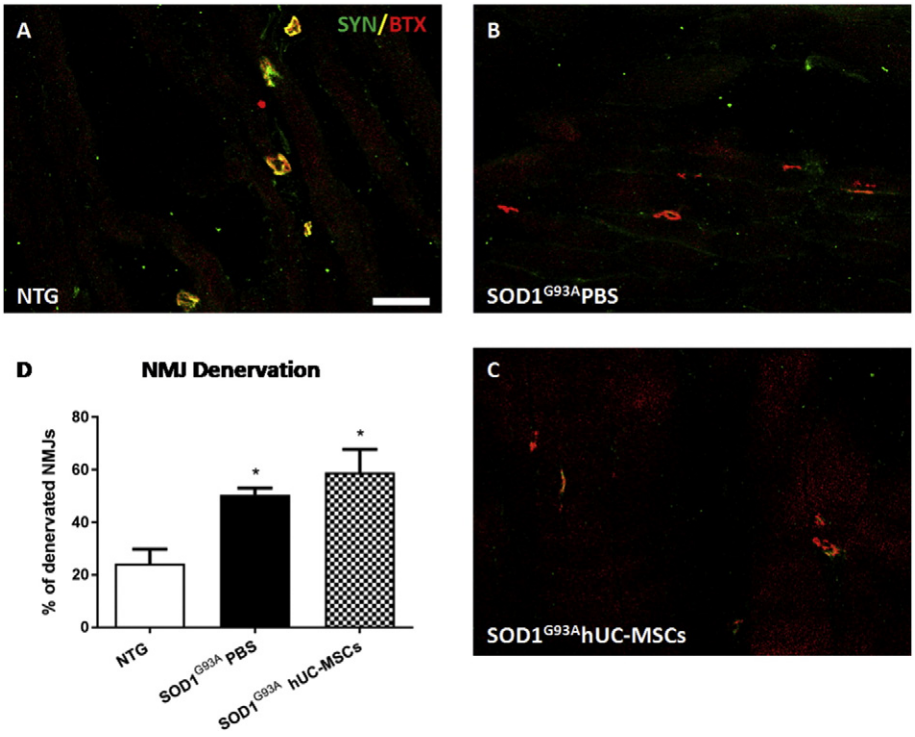

Fig. 3. Neuromuscular junction denervation. Neuromuscular junction denervation was evaluated by immunohistochemistry in tibialis anterior muscles at symptomatic stage of the disease (140 days). Representative images of co-localization of synaptophysin (SYN, green) with bungarotoxin (BTX, red) of NTG (A), SOD1^{G93A} PBS (B) and transgenic mice treated with hUC-MSCs (C) scale bar 50 μm. Percentage of neuromuscular junction denervation was higher in tibialis anterior of SOD1^{G93A} mice respect to NTG, without any difference after the treatment with hUC-MSCs (D). Data are expressed as mean ± SEM, ($n = 4$ animals). Statistical analysis was performed using One way ANOVA, followed by post-hoc Tukey's test (p value < 0.05 vs NTG).

disease and protecting motor neurons in SOD1G93A mice, even if with a certain variability in relation to the dose and route of administration (Lewis and Suzuki, 2014; Zhijuan Mao and Chen, 2015). In this study, hUC-MSCs were selected for their lower risk of rejection compared to other stem cells, therefore UC results a more appealing cell source for application in an allogeneic system. We decided to evaluate the effect of repeated administration of hUC-MSCs since our previous results (Violatto et al., 2015) showed that after a single ICV injection the number of cells that remained longer in the ventricles was limited and only very few cells migrated into the spinal cord one week after the injection. In line with this, here we observed that the size and the number of cell clusters confined to the third ventricle were markedly decreased 6 weeks after a single injection and no cells were detected in the spinal cord. Instead, after the second and third administration the size and the number of cell clusters appeared higher in the ventricles, nevertheless the presence of cells in the brain or spinal cord parenchyma was not detected. This suggests that the hUC-MSCs have low capacity of migration and engraftment, therefore their beneficial effect in protecting the motor neurons and reduce microgliosis in the lumbar spinal cord can only be associated with a paracrine effect. Such phenomenon has been suggested also for the neuroprotective effect induced by MSCs from other sources and delivered intrathecally (Boido et al., 2014; Habisch et al., 2007; Vercelli et al., 2008).

Several pieces of evidence suggest that MSCs may exert a protective role on motor neurons in SOD1G93A mice modifying the inflammatory milieu of the host spinal cord (Boido et al., 2014). In agreement with this, we found that while the transcription of endogenous murine pro-inflammatory cytokines, IL-6 and IL-1β, was partially decreased, the mRNA levels of anti-inflammatory cytokines such as IL-4, and at a lower level IL-10, were higher in the spinal cord of mice treated with hUC-MSCs compared to the PBS-treated SOD1G93A mice. These results indicate a clear shift towards an anti-inflammatory environment. This is consistent with the attenuation of the activated microglia and a probable shift from a classically activated M1 phenotype toward an alternative activated or deactivated M2 phenotype with neuroprotective function, as previously suggested from in vitro and in vivo model of ALS (Henkel et al., 2009; Zhao et al., 2010). In fact, it has been proposed that while IL-10 may induce an M2 deactivated polarization state of microglia, IL-4 generates an M2-alternatively activated polarized phenotype. M2 microglia in turn may block the release of pro-inflammatory cytokines and secrete high levels of IL-4, IL-10, and IGF-1, all of which may enhance neuronal survival (Henkel et al., 2009). Interestingly, in addition to IL-4, we also found a marked upregulation of IGF-1 in the spinal cord of hUC-MSCs-treated mice with respect to the vehicle group. IGF-1 administered through viral delivery either intramuscular (Kaspar, 2003) or intraparenchymal (Lepore et al., 2007) or by intrathecal administration (Nagano et al., 2005) has been reported to have a neuroprotective effect in ALS mouse models and this effect was associated with increased levels of p-Akt in the spinal cord homogenate (Kaspar, 2003; Nagano et al., 2005). Consistently, here we found that treatment with hUC-MSCs increased the levels of p-Akt in the spinal cord homogenate providing a further evidence for the neuroprotective efficacy in SOD1G93A mice. Moreover, for the first time, we demonstrate that treatment with hUC-MSCs activated the p-Akt pathway not only in the MNs but above all, in the reactive astrocytes, which promote neuron survival. This is consistent with the increase of GFAP immunoreactivity in the lumbar spinal cord of SOD1G93A mice treated with hUC-MSCs. This effect is probably mediated by the augmented transcription of IGF-1. In fact, studies in vitro have demonstrated that IGF-1 is a potent activator of p-Akt in mutant SOD1 MN-astrocytes coculture and this is a key mechanism for IGF-1 to induce neuroprotection against oxidative stress injury (Dávila et al., 2016). Thus, it is possible that even in the presence of the pro-oxidant SOD1G93A, the activated astrocytes in the spinal cord of hUC-MSC treated mice may acquire a neuroprotective function through the activation of the IGF-1-p-Akt pathway (Dávila et al., 2016).

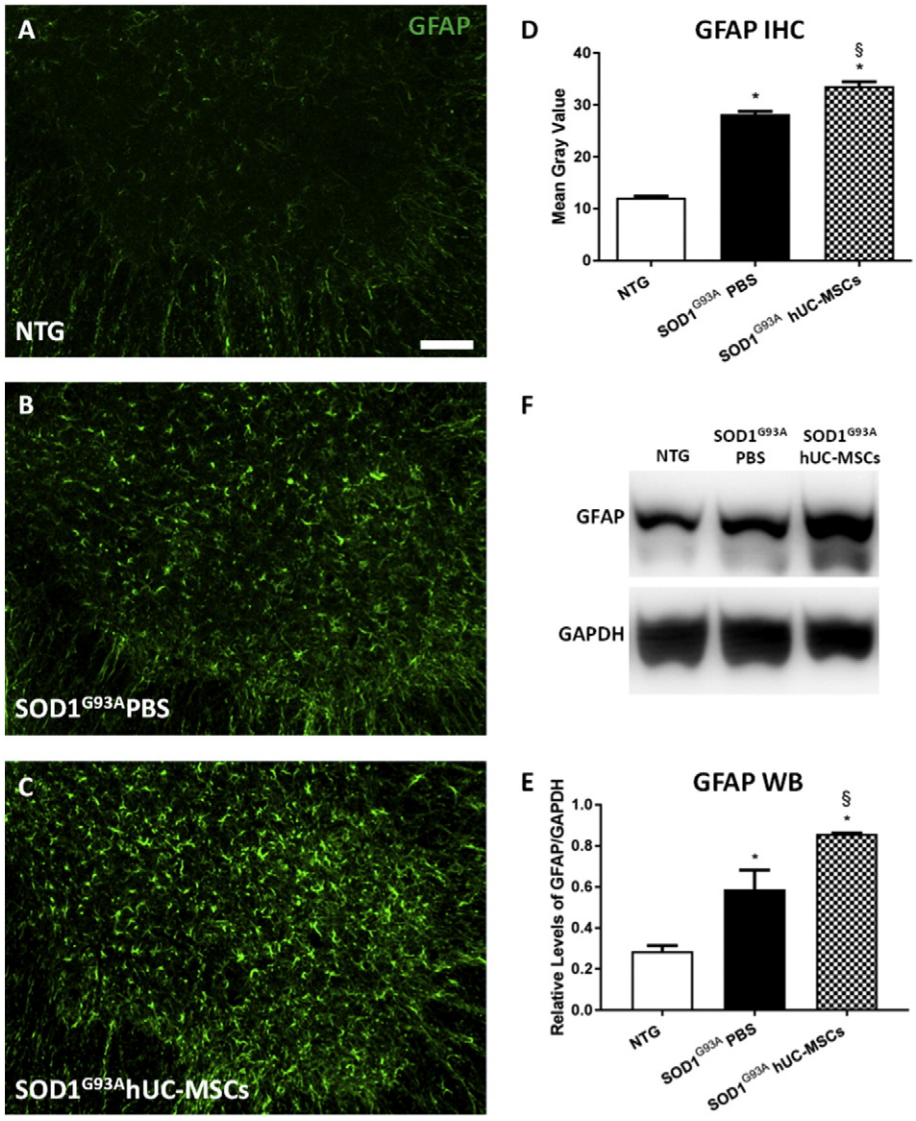

Fig. 4. Evaluation of reactive astrocytosis. Representative images of ventral lumbar spinal cord hemisections stained with GFAP (green) at 140 days of age (A-C) scale bar 50 μm. Quantification of immunofluorescence showed elevated astrocytosis in the ventral horn of SOD1^{G93A} mice at the symptomatic stage of the pathology as compared to NTG. Treatment with hUC-MSCs significantly increases the reactive astrocytosis (D). Bar graph are mean ± SEM as a percentage versus NTG controls ($n = 4$–5 animals for each group). Statistical analysis was performed using One Way ANOVA followed by post hoc Tukey test; * = $p < 0.0001$ vs NTG; § = $p < 0.0001$ vs SOD1G93APBS. Representative GFAP immunoblots performed on the lumbar spinal cord of NTG and transgenic mice treated with PBS or hUC-MSCs, at 140 days of age (E), and relative quantification (F). Bar represents mean ± SEM as a percentage versus NTG controls ($n = 4$ animals per group). Data were analyzed using One way ANOVA followed by post hoc Tukey test; * = $p < 0.001$ vs NTG; § = $p < 0.05$ vs SOD1^{G93A}PBS.

Another study evaluating the effect of MSCs derived from human adipose tissue in SOD1G93A mice reported increased levels of IGF-1 in the spinal cord in addition to other neurotrophic factors (BDNF, GDNF, CNTF) (Kim et al., 2014). Interestingly, Jeon and colleagues (Jeon et al., 2016) using the cytosolic extract of human adipose stem cells (hASC) demonstrated a significant neuroprotective effect on MN, that is associated with an increased expression of p-Akt, p-CREB, and PGC-1α in SOD1G93A mouse model. Thus, together with this observation, our data suggest that the activation of p-Akt induced by IGF-1 in both motor neurons and astrocytes play an important role in the neuroprotective action of MSCs secretome.

Of note, in the present study, the reduced loss of motor neurons is not associated with a preservation of the innervated neuromuscular junction with the consequence of a lack of beneficial effect on the progression of the disease in SOD1G93A mice. Other studies have reported similar results in these mice either with cell therapy or other interventions. For example, transplantation of Sertoli cells into the parenchyma of the lumbar spinal cord significantly protects motor neurons in SOD1G93A mice without modifying the disease onset neither the survival (Hemendinger et al., 2005). Likewise, treatment with sodium valproate, which did exert a neuroprotective effect in SOD1G86R mice, was unable to extend the mean survival of ALS mice, because it did not ameliorate skeletal muscle denervation (Rouaux et al., 2007). Another example refers to the intraparenchymal spinal cord delivery of adeno-associated virus IGF-1 (Lepore et al., 2007). In fact, while the treatment with AAV2-IGF-1 delayed the disease onset and extended survival in male SOD1G93A mice, this effect was not detected in female SOD1G93A despite a similar protection of spinal motor neurons. This observation was confirmed by another group who delivered the same AVV2-IGF-1 in the rat SOD1G93A (Franz et al., 2009). They observed a significant protection of motor neurons after intraspinal cord delivery of IGF-1, however only in males there was a partial amelioration of the grip strength, which was not sufficient to delay the onset and to increase the duration of the disease in both male and female rats. Noteworthy, another group using human hUC-MSC injected directly into the lumbar spinal cord of male and female SOD1G93A mice also

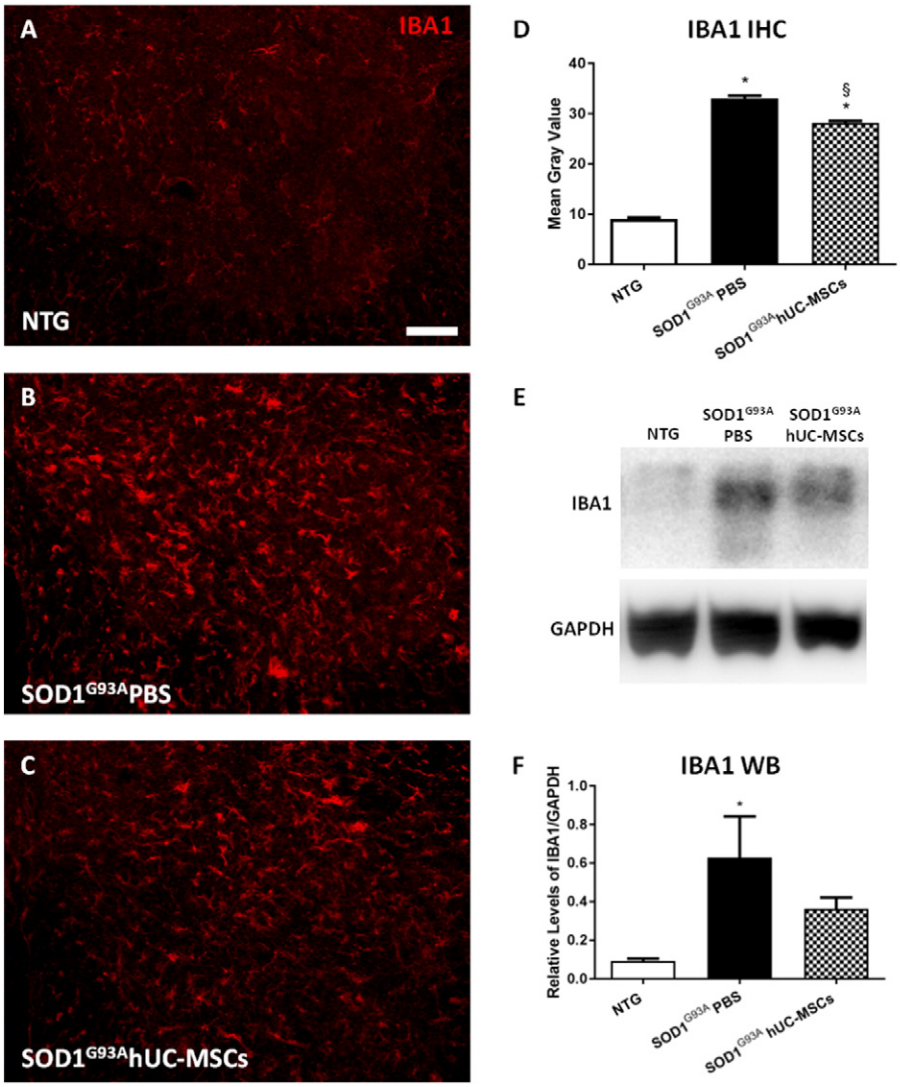

Fig. 5. Evaluation of reactive microgliosis. Representative images of ventral lumbar spinal cord hemisections stained with IBA1 (red) at 140 days of age (A–C) scale bar 50 μm. IBA1 immunofluorescence was decreased in mice treated with MSC compared to vehicle group at 140 days of age. Bar graphs are mean ± SEM as a percentage versus NTG controls ($n = 4$–5 animals for each group). Statistical analysis was performed using One Way ANOVA followed by post hoc Tukey test; * = $p < 0.0001$ vs NTG; § = $p < 0.0001$ vs SOD1^{G93A}PBS. Representative IBA1 immunoblots performed on the lumbar spinal cord at 140 days of age (E), and relative quantification (F). Bar represents mean ± SEM ($n = 4$ animals per group). Data were analyzed using One way ANOVA followed by post hoc Tukey test; * = $p < 0.05$ vs NTG.

reported a significant MN protection in the lumbar spinal cord of both genders with a significant improvement of Rota-Rod and PaGE performance only in male mice (Vercelli et al., 2008). Since in the present study we used only female SOD1G93A mice this may have prevented us from observing a beneficial effect on the disease progression, even in presence of a significant neuroprotection. The mechanism for which the effect is restricted to male is unknown, but the authors suggested that the differences in disease progression, sex hormones and/or levels and sensitivity of components of the IGF-1 system may be the cause of this discrepancy (Lepore et al., 2007). However, this hypothesis deserves further investigation.

On the contrary, Zhang et al. (2009) which did multiple deliveries of BM-MSC confined to the cerebral ventricles only in female SOD1G93A mice, showed a beneficial effect on the disease progression in association to MNs protection. They began their first treatment at the early pre-symptomatic stage (8weeks of age) and this may be relevant to the protection of the NMJs, since it has been suggested that alterations in distal motor axons are the earliest pathological changes in the pathogenesis of ALS, followed by a "dying back" process (Fischer et al., 2004). Thus, in the Zhang's study the growth factors produced and secreted by cells in the CSF may have more time to reach the peripheral nervous system and to improve the function of the NMJs. In addition, in Zhang's study the number of cells injected was double than those administered in our study and, importantly, the survival rate of hUC-MSCs in CSF seems to be lower than that of BM-MSCs (Habisch et al., 2007). This suggests that transplanting stem cells in periphery might have more impact on the disease progression in SOD1G93A mice. In fact, there are several studies showing delay in disease progression and increased survival of SOD1G93A mice after intravenous injection of MSCs from different sources (Kim et al., 2014; Sun et al., 2014; Zhao et al., 2007). A disadvantage of the peripheral administration is that it requires a huge amount of cells to be injected and since most of them end up in the lungs and the liver to be expelled, this can cause serious side effects.

5. Conclusion

In summary, this study shows that intracerebroventricular transplanted hUC-MSC partially prevent the spinal MNs loss and this effect is probably linked to the activation by IGF-1 of the p-Akt survival pathway in both MN and in protective reactive astrocytes. This study further strengthens the hypothesis that the protective effect of hUC-

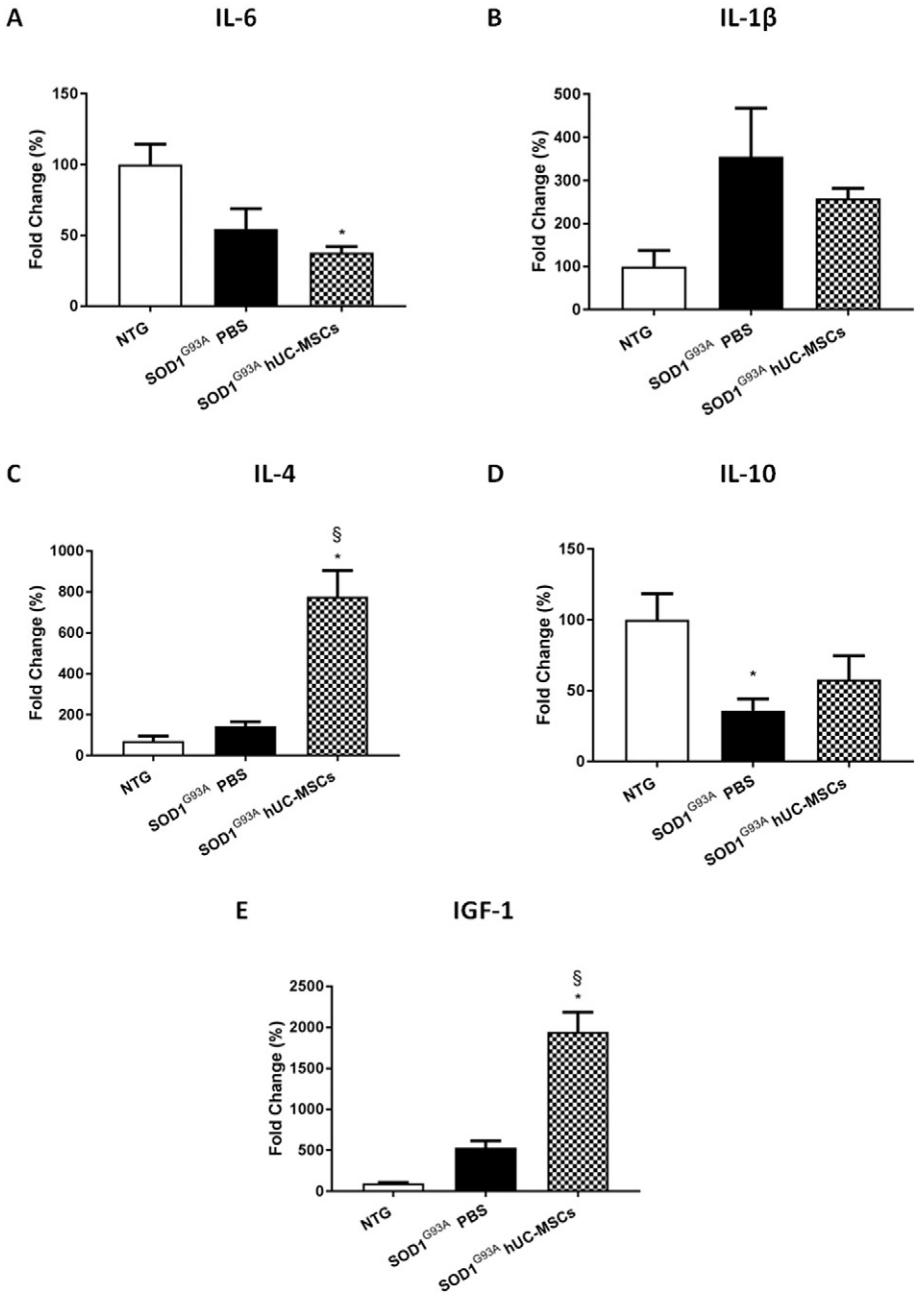

Fig. 6. Evaluation of pro- and anti-inflammatory cytokines and IGF-1. Real-time PCR reveals that mRNA levels of pro-inflammatory cytokines IL-6 (A) and IL-1β (B) tended to in hUC-MSCs-treated mice compared to the group treated with PBS (* = $p < 0.05$ vs NTG). mRNA levels of pro-inflammatory cytokine IL-4 (C) strongly increased in hUC-MSCs-treated mice compared to the group treated with PBS (*$p < 0.001$ vs NTG; § = $p < 0.001$ vs SOD1G93A PBS) and IL-10 (D) decreased in PBS-treated mice compared to NTG, while in mice treated with hUC-MSCs tended to increase (* = $p < 0.05$ vs NTG). Furthermore, mRNA levels of the IGF-1 strongly increased in hUC-MSCs-treated mice compared to the group treated with PBS (*$p < 0.001$ vs NTG; § = $p < 0.001$ vs SOD1G93A PBS). Bar graphs are mean ± SEM as a percentage versus NTG controls ($n = 4$–5 animals for each group).

MSCs is not due to cell replacement but to a shift from a pro-inflammatory (IL-6, IL-1β) to anti-inflammatory (IL-4, IL-10) and neuroprotective (IGF-1) environment in the lumbar spinal cord. However, it also emphasizes that the protection of the motor neuron perikarya in the spinal cord is not a condition sufficient to prevent the muscle denervation and thereby to delay the disease progression. This agrees with emerging findings that the preservation and the maintenance of functional peripheral nervous system through its interaction with immune response is essential for delaying disease progression in SOD1G93A mouse model and potentially to ALS patients. Thus, an integrated approach which combines a neuroprotective treatment with the preservation of the peripheral motor axons and NMJs should increase the efficacy of ALS therapy.

Ethics approval

For the umbilical cord informed written consent was obtained from each donor mother according to the guidelines of the ethical committee of the ASST Papa Giovanni XXIII. All procedures performed in the study involving animals were in accordance with the ethical standards of the Mario Negri Institute at which the studies were conducted. Procedure involving animals and their care were conducted in according to the institutional guidelines, that are in compliance with national (D.lgs 26/2014; Authorization n.19/2008-A issued March 6, 2008 by Ministry of Health) and international laws and policies (EEC Council Directive 2010/63/UE; NIH Guide for the Care and use of Laboratory Animals, U.S. National Research Council, 2011 edition). This specific protocol

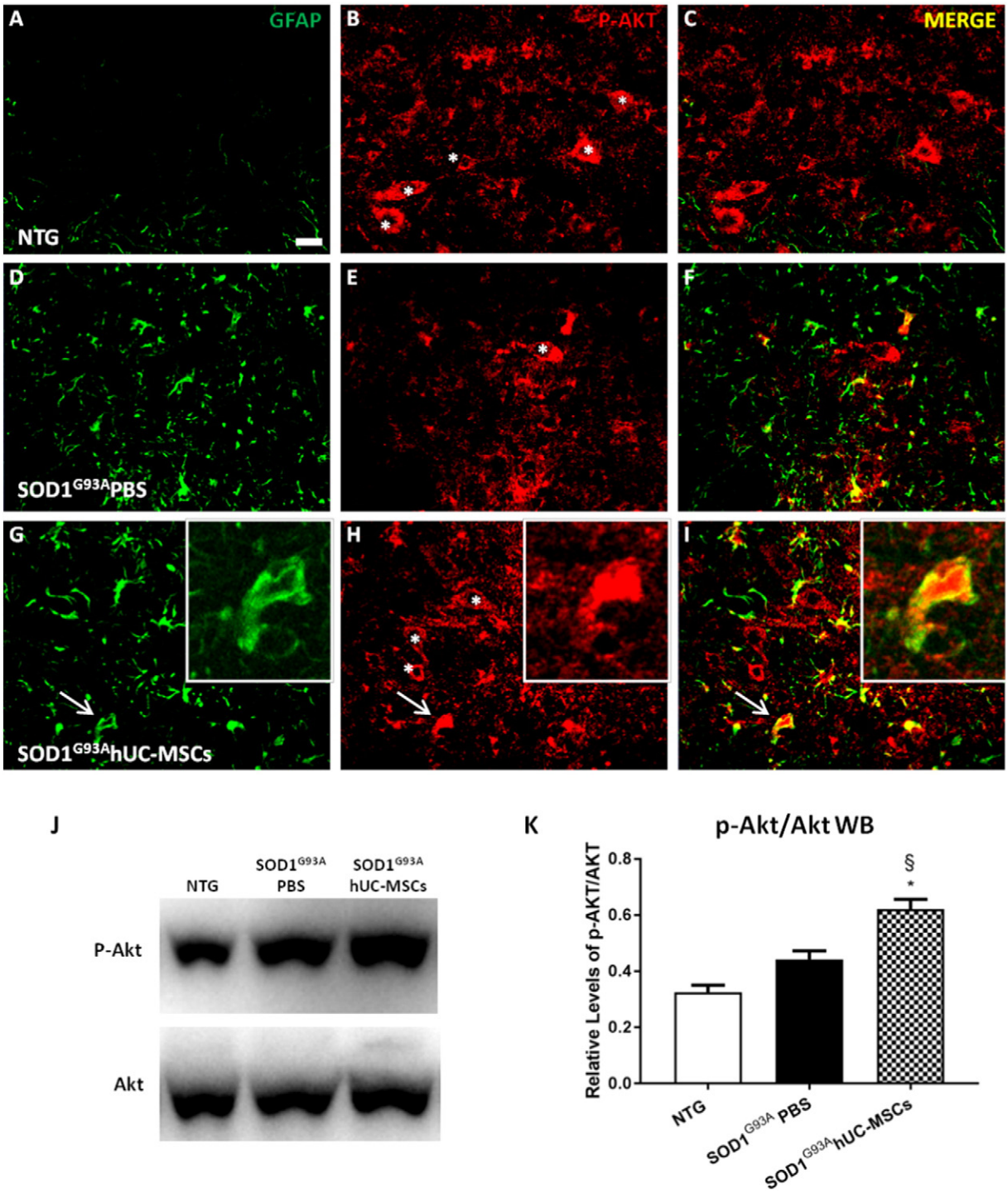

Fig. 7. Activation of p-Akt pro-survival pathway. Panels A–I laser scanning confocal microphotographs of p-Akt (red, A, D, G) and GFAP (green signal in B, E, H) in the ventral horn of lumbar spinal cord of SOD1G93A mice at symptomatic stage of the disease, compared to NTG littermates. In SOD1G93A mice we observed that hypertrophic astrocytes were co-stained with p-Akt signal (arrow), that are in greater number in mice treated with hUC-MSCs. P-AKT immunoreactivity is also present in cells that, morphologically, we can recognize as motor neurons (asterisks, B, E, H). Representative immunoblots performed on the lumbar spinal cord of transgenic mice treated with PBS or hUC-MSCs, at 140 days of age, and relative quantification. There was a slight but significant increase of Akt phosphorylation (at Ser473) in mice treated with hUC-MSCs. Bar represents mean ± SEM ($n = 4$ animals per group). Data were analyzed using One way ANOVA followed by post hoc Tukey test; * = $p < 0.001$ vs NTG; § = $p < 0.01$ vs SOD1G93A PBS.

was approved by IRCCS-IRFMN Animal Care and Use Committee (IACUC) and then approved by the Italian "Istituto Superiore di Sanità" (code: N° 1131/2015 PR).The 3R principles and ARRIVE guidelines have been considered at each stage of the experimental planning. In this regard, the experiments have been designed so that the minimum number of animals required for reliable statistical analysis have been used. Animals with substantial motor impairment received food on the cage bottom and water bottles with long drinking spouts and all animals for in vivo analysis were deeply anesthetized before the sacrifice.

Consent for publication

Not applicable.

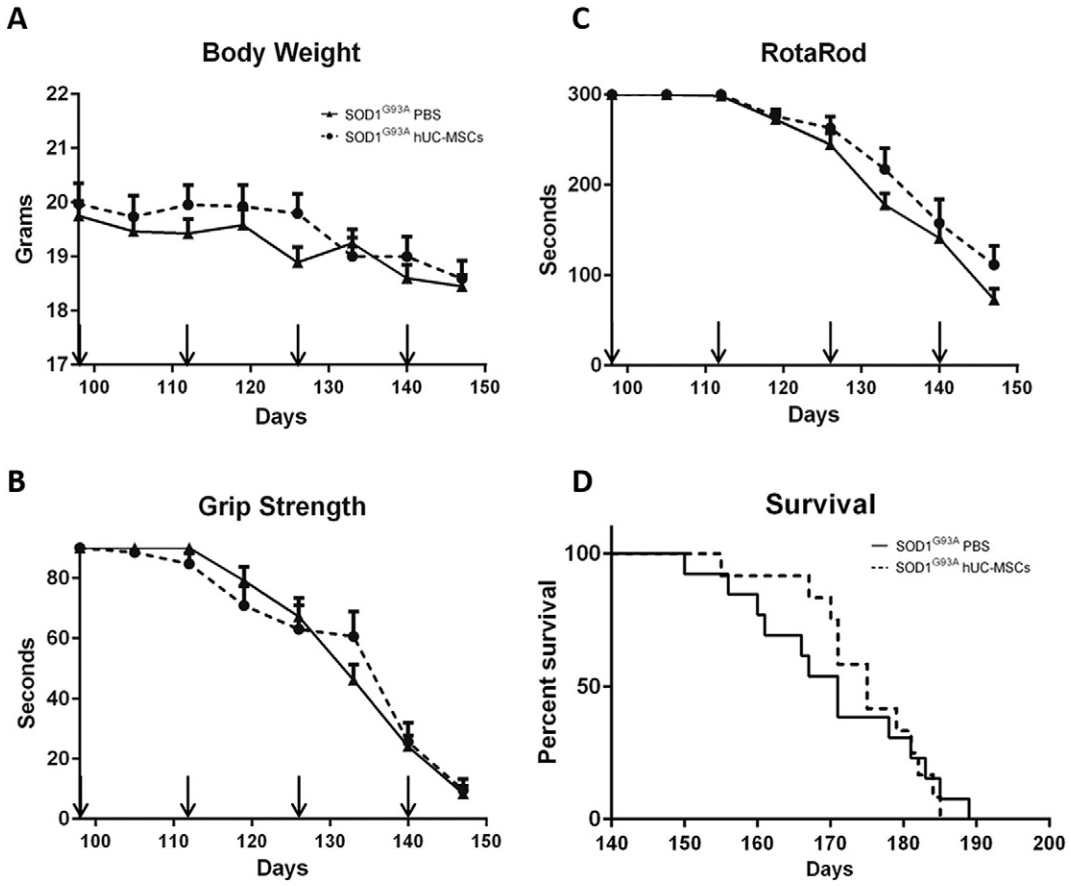

Fig. 8. Behavioral analysis and survival. The ICV treatment with hUC-MSCs showed no significant changes in weight loss (A) or improvement of motor performance in paw grip endurance test (B) and in the Rota-Rod test (C) compared to SOD1^{G93A} mice treated with PBS. The arrows are in correspondence of repeated treatments. Each point in the curves represents the mean ± SEM ($n = 14–15$). Data were analyzed by Two Way ANOVA for repeated measures, followed by post-hoc Tukey's test. The treatment with stem cell showed no changes in survival extension (D) compared to SOD1G93A mice treated with vehicle. The curve was evaluated by the Log-rank test, $p = 0.8906$; chisquare = 0.01891 ($n = 12–15$).

Availability of data and materials

All data generated or analyzed during this study are included in this published article.

Competing interests

The authors declare that they have no competing interests.

Funding

This work was supported by associazione “Amici del Mario Negri”, Fondazione Italiana di Ricerca per la Sclerosi Laterale Amiotrofica (AriSLA)-Animal Facility. Support from Associazione Italiana Lotta alle Leucemie, Linfomi e Mieloma — sezione Paolo Belli and FP7-HEALTH-2012-INNOVATION-1 (grant 305436, Stellar project) was given to CC and MI.

Authors' contributions

CC, MBV and LT conducted all the procedures involving the human UC-MSCs cultures. FS and MF performed the ICV treatment. DM and AA performed nanoparticle synthesis. MBV and LT executed cell labeling and tracking analysis. FS, AV, RDG and MT conducted the behavioral analysis, the recruitment of the mouse tissues, the immunohistochemical and biochemical analysis of the spinal cord and muscles. CB, PB and MI supervised and designed the experiments. FS, AV and CB wrote the manuscript. All authors have read and edited the manuscript and approved the final version.

Acknowledgements

Not applicable.

References

Adami, R., Scesa, G., Bottai, D., 2014. Stem cell transplantation in neurological diseases: improving effectiveness in animal models. Front. Cell Dev. Biol. 2, 17. https://doi.org/10.3389/fcell.2014.00017.

Bendotti, C., Carrì, M.T., 2004. Lessons from models of SOD1-linked familial ALS. Trends Mol. Med. 10, 393–400.

Bigini, P., Veglianese, P., Andriolo, G., Cova, L., Grignaschi, G., Caron, I., Daleno, C., Barbera, S., Ottolina, a., Calzarossa, C., Lazzari, L., Mennini, T., Bendotti, C., Silani, V., 2011. Intracerebroventricular administration of human umbilical cord blood cells delays disease progression in two murine models of motor neuron degeneration. Rejuvenation Res. 14:623–639. https://doi.org/10.1089/rej.2011.1197.

Bigini, P., Zanier, E.R., Saragozza, S., Maciotta, S., Romele, P., Bonassi Signoroni, P., Silini, A., Pischiutta, F., Sammali, E., Balducci, C., Violatto, M.B., Talamini, L., Garry, D., Moscatelli, D., Ferrari, R., Salmona, M., De Simoni, M.G., Maggi, F., Simoni, G., Grati, F.R., Parolini, O., 2016. Internalization of nanopolymeric tracers does not alter characteristics of placental cells. J. Cell. Mol. Med. 20:1036–1048. https://doi.org/10.1111/jcmm.12820.

Boido, M., Piras, A., Valsecchi, V., Spigolon, G., Mareschi, K., Ferrero, I., Vizzini, A., Temi, S., Mazzini, L., Fagioli, F., Vercelli, A., 2014. Human mesenchymal stromal cell transplantation modulates neuroinflammatory milieu in a mouse model of amyotrophic lateral sclerosis. J. Cytotherapy 16:1059–1072. https://doi.org/10.1016/j.jcyt.2014.02.003.

Brunet, A., Datta, S.R., Greenberg, M.E., 2001. Transcription-dependent and -independent control of neuronal survival by the PI3K-Akt signaling pathway. Curr. Opin. Neurobiol. https://doi.org/10.1016/S0959-4388(00)00211-7.

Capelli, C., Gotti, E., Morigi, M., Rota, C., Weng, L., Dazzi, F., Spinelli, O., Cazzaniga, G., Trezzi, R., Gianatti, A., Rambaldi, A., Golay, J., Introna, M., 2011. Minimally manipulated whole human umbilical cord is a rich source of clinical-grade human mesenchymal stromal cells expanded in human platelet lysate. Cytotherapy 13, 786–801.

Capelli, C., Pedrini, O., Valgardsdottir, R., Da Roit, F., Golay, J., Introna, M., 2015. Clinical grade expansion of MSCs. Immunol. Lett. 168:222–227. https://doi.org/10.1016/j.imlet.2015.06.006.

Caron, I., Micotti, E., Paladini, A., Merlino, G., Plebani, L., Forloni, G., Modo, M., Bendotti, C., 2015. Comparative magnetic resonance imaging and histopathological correlates in two SOD1 transgenic mouse models of amyotrophic lateral sclerosis. PLoS One 10: 1–19. https://doi.org/10.1371/journal.pone.0132159.

Cleveland, D.W., Rothstein, J.D., 2001. From Charcot to Lou Gehrig: deciphering selective motor neuron death in ALS. Nat. Rev. Neurosci. 2:806–819. https://doi.org/10.1038/35097565.

Coatti, G.C., Beccari, M.S., Olávio, T.R., Mitne-Neto, M., Okamoto, O.K., Zatz, M., 2015. Stem cells for amyotrophic lateral sclerosis modeling and therapy: myth or fact? Cytom. Part A 87:197–211. https://doi.org/10.1002/cyto.a.22630.

Dávila, D., Fernández, S., Torres-Alemán, I., 2016. Astrocyte resilience to oxidative stress induced by insulin-like growth factor i (IGF-I) involves preserved AKT (protein kinase B) activity. J. Biol. Chem. https://doi.org/10.1074/jbc.M115.695478.

Dossi, M., Ferrari, R., Dragoni, L., Martignoni, C., Gaetani, P., D'Incalci, M., Morbidelli, M., Moscatelli, D., 2013. Synthesis of fluorescent PMMA-based nanoparticles. Macromol. Mater. Eng. 298:771–778. https://doi.org/10.1002/mame.201200122.

Fischer, L.R., Culver, D.G., Tennant, P., Davis, A.A., Wang, M., Castellano-Sanchez, A., Khan, J., Polak, M.A., Glass, J.D., 2004. Amyotrophic lateral sclerosis is a distal axonopathy: evidence in mice and man. Exp. Neurol. 185, 232–240.

Franz, C.K., Federici, T., Yang, J., Backus, C., Oh, S.S., Teng, Q., Carlton, E., Bishop, K.M., Gasmi, M., Bartus, R.T., Feldman, E.L., Boulis, N.M., 2009. Intraspinal cord delivery of IGF-I mediated by adeno-associated virus 2 is neuroprotective in a rat model of familial ALS. Neurobiol. Dis. https://doi.org/10.1016/j.nbd.2008.12.003.

Garbuzova-Davis, S., Rodrigues, M.C.O., Mirtyl, S., Turner, S., Mitha, S., Sodhi, J., Suthakaran, S., Eve, D.J., Sanberg, C.D., Kuzmin-Nichols, N., Sanberg, P.R., 2012. Multiple intravenous administrations of human umbilical cord blood cells benefit in a mouse model of ALS. PLoS One 7. https://doi.org/10.1371/journal.pone.0031254.

Glass, J.D., Hertzberg, V.S., Boulis, N.M., Riley, J., Federici, T., Polak, M., Bordeau, J., Fournier, C., Johe, K., Hazel, T., Cudkowicz, M., Atassi, N., Borges, L.F., Rutkove, S.B., Duell, J., Patil, P.G., Goutman, S.A., Feldman, E.L., 2016. Transplantation of spinal cord-derived neural stem cells for ALS: analysis of phase 1 and 2 trials. Neurology https://doi.org/10.1212/WNL.0000000000002889.

Habisch, H.J., Janowski, M., Binder, D., Kuzma-Kozakiewicz, M., Widmann, A., Habich, A., Schwalenstöcker, B., Hermann, A., Brenner, R., Lukomska, B., Domanska-Janik, K., Ludolph, A.C., Storch, A., 2007. Intrathecal application of neuroectodermally converted stem cells into a mouse model of ALS: limited intraparenchymal migration and survival narrows therapeutic effects. J. Neural Transm. 114:1395–1406. https://doi.org/10.1007/s00702-007-0748-y.

Hemendinger, R., Wang, J., Malik, S., Persinski, R., Copeland, J., Emerich, D., Gores, P., Halberstadt, C., Rosenfeld, J., 2005. Sertoli cells improve survival of motor neurons in SOD1 transgenic mice, a model of amyotrophic lateral sclerosis. Exp. Neurol. 196:235–243. https://doi.org/10.1016/j.expneurol.2005.07.025.

Henkel, J.S., Beers, D.R., Zhao, W., Appel, S.H., 2009. Microglia in ALS: the good, the bad, and the resting. J. NeuroImmune Pharmacol. https://doi.org/10.1007/s11481-009-9171-5.

Jeon, G.S., Im, W., Shim, Y.-M., Lee, M., Kim, M.-J., Hong, Y.-H., Seong, S.-Y., Kim, M., Sung, J.-J., 2016. Neuroprotective effect of human adipose stem cell-derived extract in amyotrophic lateral sclerosis. Neurochem. Res. 41:913–923. https://doi.org/10.1007/s11064-015-1774-z.

Kaspar, B.K., 2003. Retrograde viral delivery of IGF-1 prolongs survival in a mouse ALS model. Science (80-.) https://doi.org/10.1126/science.1086137.

Kiernan, M.C., Vucic, S., Cheah, B.C., Turner, M.R., Eisen, A., Hardiman, O., Burrell, J.R., Zoing, M.C., 2011. Amyotrophic lateral sclerosis. Lancet 377:942–955. https://doi.org/10.1016/S0140-6736(10)61156-7.

Kim, H., Kim, H.Y., Choi, M.R., Hwang, S., Nam, K.H., Kim, H.C., Han, J.S., Kim, K.S., Yoon, H.S., Kim, S.H., 2010. Dose-dependent efficacy of ALS-human mesenchymal stem cells transplantation into cisterna magna in SOD1-G93A ALS mice. Neurosci. Lett. 468:190–194. https://doi.org/10.1016/j.neulet.2009.10.074.

Kim, K.S., Lee, H.J., An, J., Kim, Y.B., Ra, J.C., Lim, I., Kim, S.U., 2014. Transplantation of human adipose tissue-derived stem cells delays clinical onset and prolongs life span in ALS mouse model. Cell Transplant. 23:1585–1597. https://doi.org/10.3727/096368913X673450.

Koh, S.H., Kim, K.S., Choi, M.R., Jung, K.H., Park, K.S., Chai, Y.G., Roh, W., Hwang, S.J., Ko, H.J., Huh, Y.M., Kim, H.T., Kim, S.H., 2008. Implantation of human umbilical cord-derived mesenchymal stem cells as a neuroprotective therapy for ischemic stroke in rats. Brain Res. 1229:233–248. https://doi.org/10.1016/j.brainres.2008.06.087.

Kruminis-Kaszkiel, E., Wojtkiewicz, J., Maksymowicz, W., 2014. Glial-restricted precursors as potential candidates for ALS cell-replacement therapy. Acta Neurobiol. Exp. (Wars) 74, 233–241.

Lepore, A.C., Haenggeli, C., Gasmi, M., Bishop, K.M., Bartus, R.T., Maragakis, N.J., Rothstein, J.D., 2007. Intraparenchymal spinal cord delivery of adeno-associated virus IGF-1 is protective in the SOD1G93A model of ALS. Brain Res. https://doi.org/10.1016/j.brainres.2007.09.034.

Lewis, C.M., Suzuki, M., 2014. Therapeutic applications of mesenchymal stem cells for amyotrophic lateral sclerosis. Stem Cell Res Ther 5:32. https://doi.org/10.1186/scrt421.

Lund, R.D., Wang, S., Lu, B., Girman, S., Holmes, T., Sauvé, Y., Messina, D.J., Harris, I.R., Kihm, A.J., Harmon, A.M., Chin, F.-Y., Gosiewska, A., Mistry, S.K., 2007. Cells isolated from umbilical cord tissue rescue photoreceptors and visual functions in a rodent model of retinal disease. Stem Cells 25:602–611. https://doi.org/10.1634/stemcells.2006-0308.

Mazzini, L., Gelati, M., Profico, D.C., Sgaravizzi, G., Projetti Pensi, M., Muzi, G., Ricciolini, C., Rota Nodari, L., Carletti, S., Giorgi, C., Spera, C., Domenico, F., Bersano, E., Petruzzelli, F., Cisari, C., Maglione, A., Sarnelli, M.F., Stecco, A., Querin, G., Masiero, S., Cantello, R., Ferrari, D., Zalfa, C., Binda, E., Visioli, A., Trombetta, D., Novelli, A., Torres, B., Bernardini, L., Carriero, A., Prandi, P., Servo, S., Cerino, A., Cima, V., Gaiani, A., Nasuelli, N., Massara, M., Glass, J., Sorarù, G., Boulis, N.M., Vescovi, A.L., 2015. Human neural stem cell transplantation in ALS: initial results from a phase I trial. J. Transl. Med. 13, 371. https://doi.org/10.1186/s12967-014-0371-2.

Nagano, I., Ilieva, H., Shiote, M., Murakami, T., Yokoyama, M., Shoji, M., Abe, K., 2005. Therapeutic benefit of intrathecal injection of insulin-like growth factor-1 in a mouse model of amyotrophic lateral sclerosis. J. Neurol. Sci. https://doi.org/10.1016/j.jns.2005.04.011.

Peviani, M., Cheroni, C., Troglio, F., Quarto, M., Pelicci, G., Bendotti, C., 2007. Lack of changes in the PI3K/AKT survival pathway in the spinal cord motor neurons of a mouse model of familial amyotrophic lateral sclerosis. Mol. Cell. Neurosci. https://doi.org/10.1016/j.mcn.2007.01.003.

Peviani, M., Tortarolo, M., Battaglia, E., Piva, R., Bendotti, C., 2014. Specific induction of Akt3 in spinal cord motor neurons is neuroprotective in a mouse model of familial amyotrophic lateral sclerosis. Mol. Neurobiol. https://doi.org/10.1007/s12035-013-8507-6.

Rouaux, C., Panteleeva, I., Rene, F., Gonzalez de Aguilar, J.-L., Echaniz-Laguna, A., Dupuis, L., Menger, Y., Boutillier, A.-L., Loeffler, J.-P., 2007. Sodium valproate exerts neuroprotective effects in vivo through CREB-binding protein-dependent mechanisms but does not improve survival in an amyotrophic lateral sclerosis mouse model. J. Neurosci. 27:5535–5545. https://doi.org/10.1523/JNEUROSCI.1139-07.2007.

Rowland, Lewis P., Shneider, N.A., 2001. Amyotrophic lateral sclerosis. N. Engl. J. Med. 344:1688–1700. https://doi.org/10.1056/NEJM200105313442207.

Sun, H., Hou, Z., Yang, H., Meng, M., Li, P., Zou, Q., Yang, L., Chen, Y., Chai, H., Zhong, H., Yang, Z.Z. huyun, Zhao, J., Lai, L., Jiang, X., Xiao, Z., 2014. Multiple systemic transplantations of human amniotic mesenchymal stem cells exert therapeutic effects in an ALS mouse model. Cell Tissue Res. 357:571–582. https://doi.org/10.1007/s00441-014-1903-z.

Todeschi, M.R., El Backly, R., Capelli, C., Daga, A., Patrone, E., Introna, M., Cancedda, R., Mastrogiacomo, M., 2015. Transplanted umbilical cord mesenchymal stem cells modify the in vivo microenvironment enhancing angiogenesis and leading to bone regeneration. Stem Cells Dev. 0, 150331084235007. https://doi.org/10.1089/scd.2014.0490.

Tortarolo, M., Veglianese, P., Calvaresi, N., Botturi, A., Rossi, C., Giorgini, A., Migheli, A., Bendotti, C., 2003. Persistent activation of p38 mitogen-activated protein kinase in a mouse model of familial amyotrophic lateral sclerosis correlates with disease progression. Mol. Cell. Neurosci. 23, 180–192.

Tortarolo, M., Vallarola, A., Lidonnici, D., Battaglia, E., Gensano, F., Spaltro, G., Fiordaliso, F., Corbelli, A., Garetto, S., Martini, E., Pasetto, L., Kallikourdis, M., Bonetto, V., Bendotti, C., 2015. Lack of TNF-alpha receptor type 2 protects motor neurons in a cellular model of amyotrophic lateral sclerosis and in mutant SOD1 mice but does not affect disease progression. J. Neurochem. 135:109–124. https://doi.org/10.1111/jnc.13154.

Uccelli, A., Milanese, M., Principato, M.C., Morando, S., Bonifacino, T., Vergani, L., Giunti, D., Voci, A., Carminati, E., Giribaldi, F., Caponnetto, C., Bonanno, G., 2012. Intravenous mesenchymal stem cells improve survival and motor function in experimental amyotrophic lateral sclerosis. Mol. Med. https://doi.org/10.2119/molmed.2011.00498.

Vercelli, A., Mereuta, O.M., Garbossa, D., Muraca, G., Mareschi, K., Rustichelli, D., Ferrero, I., Mazzini, L., Madon, E., Fagioli, F., 2008. Human mesenchymal stem cell transplantation extends survival, improves motor performance and decreases neuroinflammation in mouse model of amyotrophic lateral sclerosis. Neurobiol. Dis. 31:395–405. https://doi.org/10.1016/j.nbd.2008.05.016.

Violatto, M.B., Santangelo, C., Capelli, C., Frapolli, R., Ferrari, R., Sitia, L., Tortarolo, M., Talamini, L., Previdi, S., Moscatelli, D., Salmona, M., Introna, M., Bendotti, C., Bigini, P., 2015. Longitudinal tracking of triple labeled umbilical cord derived mesenchymal stromal cells in a mouse model of amyotrophic lateral sclerosis. Stem Cell Res. https://doi.org/10.1016/j.scr.2015.06.010.

Watson, N., Divers, R., Kedar, Roshan, Mehindru, Ankur, Mehindru, Anuj, Borlongan, M.C., Borlongan, C.V., 2015. Discarded Wharton's jelly of the human umbilical cord: a viable source for mesenchymal stem cells. Cytotherapy 17:18–24. https://doi.org/10.1016/j.jcyt.2014.08.009.Discarded.

Zhang, C., Zhou, C., Teng, J.-J., Zhao, R.-L., Song, Y.-Q., Zhang, C., 2009. Multiple administrations of human marrow stromal cells through cerebrospinal fluid prolong survival in a transgenic mouse model of amyotrophic lateral sclerosis. Cytotherapy 11:299–306. https://doi.org/10.1080/14653240902806986.

Zhao, C.-P., Zhang, C., Zhou, S.-N., Xie, Y.-M., Wang, Y.-H., Huang, H., Shang, Y.-C., Li, W.-Y., Zhou, C., Yu, M.-J., Feng, S.-W., 2007. Human mesenchymal stromal cells ameliorate the phenotype of SOD1-G93A ALS mice. Cytotherapy 9:414–426. https://doi.org/10.1080/14653240701376413.

Zhao, W., Beers, D.R., Henkel, J.S., Zhang, W., Urushitani, M., Julien, J.P., Appel, S.H., 2010. Extracellular mutant SOD1 induces microglial-mediated motoneuron injury. Glia https://doi.org/10.1002/glia.20919.

Zhijuan Mao, S.Z., Chen, H., 2015. Stem cell therapy for amyotrophic lateral sclerosis. Cell Regen. https://doi.org/10.1186/s13619-015-0026-7.